

Influence of chamber misalignment on cased telescoped (CT) ammunition accuracy

D. CORRIVEAU *, C. FLORIN PETRE

Defence R&D Canada, 2459 De La Bravoure Rd., Quebec, QC G3J 1X5, Canada

Abstract

As part of a research program, it was desired to better understand the impact of the rotating chamber alignment with the barrel throat on the precision and accuracy of a novel cased telescoped (CT) ammunition firing rifle. In order to perform the study, a baseline CT ammunition chamber which was concentric with a Mann barrel bore was manufactured. Additionally, six chambers were manufactured with an offset relative to the barrel bore. These chambers were used to simulate a misaligned chamber relative to the bore axis. Precision and accuracy tests were then performed at 200 m in an indoor range under controlled conditions. For this project, 5.56 mm CT ammunition was used. As the chamber axis offset relative to the gun bore was increased, the mean point of impact was displaced away from the target center. The shift in the impact location is explained by the presence of in-bore yaw which results in lateral throw-off and aerodynamic jump components. The linear theory of ballistics is used to establish a relationship between the chamber misalignment and the resulting projectile mean point of impact for a rifle developed to fire CT ammunition. This relationship allows for the prediction of the mean point of impact given a chamber misalignment.

Crown Copyright © 2016 Production. All rights reserved.

Keywords: Cased; Telescoped; Ammunition; Aerodynamic; Jump; Accuracy

1. Introduction

The introduction of new electronic sights to increase warfighters' awareness and communication capability on the battlefield has the potential to significantly increase their effectiveness. However, these new pieces of equipment increase the weight burden that must be carried by the soldiers. This, in turn, reduces their mobility and agility.

Two areas where significant weight reduction could be achieved are the weapon system and the ammunition. In order to reduce the weight of the ammunition, several concepts are being investigated and reached a high technology readiness level. Among these, polymer cased ammunition, caseless ammunition (CL) and cased telescoped ammunition (CT) are the most promising. Using these technologies, ammo/link weight reduction of the order of 37% and 12% volume reduction could eventually be achieved [1].

For polymer cased ammunition, a standard rifle chamber can be used. However, for CL and CT ammunition a rotating or

sliding cylindrical chamber must be used for both in-line, push through feed and ejection. With such a mechanism, there exists a possibility that the rotating or sliding chamber axis be slightly misaligned with the barrel axis. If this occurs, as the projectile is propelled out of the CT ammunition casing and it enters the leade (freebore) area before the barrel engraving, the projectile axis relative to the barrel axis will be at an angle. Therefore, the projectile gets engraved in the rifling at an angle relative to the barrel axis. This misalignment or tilt of the projectile has been shown to result in a lateral throw-off at the muzzle and an aerodynamic jump.

This is significant for high-precision gun designers as the aerodynamic jump and lateral throw-off are a significant source of dispersion. In the case of a CT ammunition rifle with a misaligned chamber, it is believed that this would affect the accuracy of the rifle in the form of a bias in the mean impact point and to a lesser extent the precision. This is explained by the fact that in the case of a misaligned chamber, the projectile would generally be always tilted in the same direction as it gets engraved after exiting the chamber.

In order to reduce the bias and the dispersion associated with the aerodynamic jump and the lateral throw-off, the gun's twist rate can be reduced to lower the spin rate of the projectile at the

Peer review under responsibility of China Ordnance Society.

* Corresponding author. Tel.: +1 4188444000.

E-mail address: daniel.corriveau@drdc-rddc.gc.ca (D. CORRIVEAU).

Nomenclature

CG_N	distance from nose to center of mass, cal
$C_{L\alpha}$	lift force coefficient
$C_{M\alpha}$	pitching moment coefficient
d	projectile caliber, m
i	$\sqrt{-1}$
I_y	transverse moment of inertia, $\text{kg}\cdot\text{m}^2$
I_x	axial moment of inertia, $\text{kg}\cdot\text{m}^2$
J_A	aerodynamic jump, rad
k^y	$\frac{I_y}{md^2}$
k^x	$\frac{I_x}{md^2}$
L_N	projectile ogive length, cal
L_{CYL}	projectile cylindrical section length, cal
m	projectile mass, kg
n	gun twist rate, cal/turn
P	spin rate, rad/sec
P	dimensionless spin rate
s	dimensionless distance
S_g	gyroscopic stability factor
t	time, sec
T_L	lateral throw-off, rad
V	projectile speed, m/sec
$\bar{\alpha}$	total incidence, deg
δ_{\max}	first maximum yaw angle, deg
ξ_0	initial complex yaw at the muzzle, rad
$\dot{\epsilon}_0$	initial yaw rate at the muzzle, rad/sec
ϵ	in-bore yaw angle, rad
$\hat{\epsilon}$	static unbalance, cal
ϕ_0	initial roll angle at the muzzle, rad

muzzle. However, for the projectile to remain gyroscopically stable, the spin rate must be kept high enough such that the gyroscopic stability factor, S_g , remains above 1 for all firing conditions.

Lateral throw-off of a projectile was first studied by Mann [2] using statically unbalanced projectiles having a center of mass off the axial axis. The aerodynamic jump was also investigated by Mann [2] using dynamically unbalanced projectile.

Murphy [3] studied a yaw induction technique for spin-stabilized projectiles using mass asymmetry. He developed a mathematical relationship that relates the size of the tricyclic arm and the dynamic unbalance due to a slight mass asymmetry.

More recently, Ritter [4] and Beyer and Ritter [5] used a custom made small caliber gun breech to quantify the initial motion of unmodified small caliber projectiles. In studying videos of the projectile at the tube exit, they observed considerable off-axis motion. Additional experiments to study and understand the implications of this motion are being developed by the authors.

In-bore yaw effects on lateral throw-off and aerodynamic jump for small caliber projectiles were also studied by

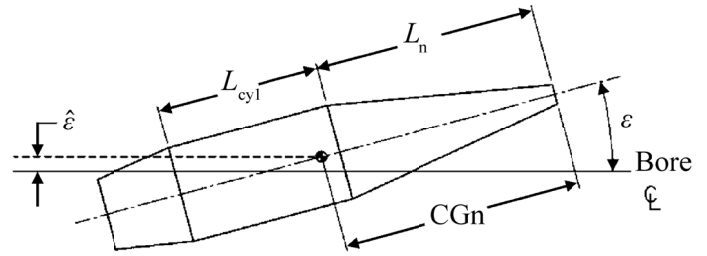


Fig. 1. Nomenclature for a projectile with in-bore yaw (adapted from McCoy [8]).

Gkritzapis and Panagiotopoulos [6] for firing sidewise from air vehicles. They used a modified linear 6-DOF flight simulation code to predict the bullet trajectory. The coupled epicyclic pitching and yawing motion of the first 100 m of the trajectories studied are used for their analysis.

As part of a research program, it was desired to better understand the impact of the rotating or sliding chamber alignment with the barrel throat on the precision and accuracy of the weapon system. In the first part of the paper, the linear theory of ballistics is used to develop a relationship between the CT ammunition projectile in-bore tilt due to chamber misalignment and the mean impact point location on a target.

The second part of the paper presents the experimental setup that was developed to verify the effect of the chamber misalignment on the precision and accuracy of the weapon system. The experimental results are then presented for the various cases studied. Finally, the prediction obtained using the theoretical relationship, developed as part of this project, is compared to the experimental results.

2. Analytical model

Using the linear theory of ballistics, an analytical model was developed in order to predict the projectile deflection at the target given a chamber misalignment or projectile in-bore tilt. The relationship was developed based on the work of Murphy [7] on the linearized swerving motion of rotationally symmetric projectiles. In developing the model, the total incidence of the projectile was assumed to be small (i.e. $\alpha < 15^\circ$). The projectile is assumed to be rotationally symmetric both in shape and mass distribution. As the projectile exits the misaligned chamber to enter the gun barrel, it gets tilted. The tilt is assumed to persist as the projectile gets engraved into the rifling of the barrel. Further assuming no bouncing or balloting of the projectile, its axis of symmetry follows a precession motion around the axis of the gun.

The tilted bullet is illustrated in Fig. 1. The in-bore yaw is labeled ϵ . The initial complex yaw at the muzzle is given by

$$\xi_0 = (\sin \epsilon) e^{i\phi_0} \quad (1)$$

where $e^{i\phi_0} = \cos \phi_0 + i \sin \phi_0$.

The initial roll angle at the muzzle, ϕ_0 , is the angle between the vertically upward plane and the plane containing both the in-bore yaw and the bore axis.

The initial yaw rate or angular velocity of the tilted projectile at the muzzle ξ_0 is caused by its spin. The initial yaw rate is the product of the spin rate and the sine of the in-bore yaw

$$\dot{\xi}_0 = ip(\sin \varepsilon)e^{i\phi_0} \quad (2)$$

The independent variable in Eq. (2) can be changed from the time to the dimensionless distance, s , using the following relationship

$$s = \frac{1}{d} \int_0^t V dt \quad (3)$$

Substituting Eq. (3) into Eq. (2), the initial rate becomes

$$\dot{\xi}_0 = \left(\frac{pd}{V} \right) \sin \varepsilon e^{i\phi_0} = i \left(\frac{2\pi}{n} \right) \sin \varepsilon e^{i\phi_0} \quad (4)$$

where n is the rifle barrel twist rate in calibers/turn.

The generalized aerodynamic jump equation was derived by Murphy [7] and only the final result is reproduced here for brevity

$$J_A = k^2 \left(\frac{C_{L\alpha}}{C_{M\alpha}} \right) i P \xi_0 \quad (5)$$

where $k^2 = \frac{C_{M\alpha}}{C_{L\alpha}} \frac{I_y}{md^2}$ and $P = \frac{I_x}{I_y} \left(\frac{pd}{V} \right)$. $C_{L\alpha}$ is the lift force

coefficient and $C_{M\alpha}$ is the pitching moment coefficient.

Substituting the equations for the initial yaw and initial yaw rate in the generalized aerodynamic jump equation, one obtains the relationship for the aerodynamic jump of a projectile with in-bore yaw

$$J_A = -i \left(\frac{2\pi}{n} \right) (k^2 - k^2) \left(\frac{C_{L\alpha}}{C_{M\alpha}} \right) \sin \varepsilon e^{i\phi_0} \quad (6)$$

$$\left(\frac{2\pi}{n} \right) \left(\frac{C_{L\alpha}}{C_{M\alpha}} \right) \sin \varepsilon e^{i\phi_0}$$

The aerodynamic jump can easily be determined provided the in-bore yaw, ε , is known. The in-bore yaw can be approximated geometrically by considering a projectile exiting a misaligned chamber and engaging in the rifling of a barrel. However, the method was found to yield non-satisfactory results and was not used for the present study. Alternatively, the in-bore yaw could have been estimated using orthogonal cameras at the muzzle during the firing. This option was not retained for the trial. In planning for this trial, it was decided to locate to high-speed orthogonal camera in the vicinity of the expected first maximum yaw for the 5.56 mm projectile. More details on the experimental setup will be given in the following section.

Having the first maximum yaw associated with each projectile, it is possible to compute the in-bore yaw angle using Kent's equation. Kent's equation derivation was first published by

Solving Eq. (7) for the in-bore yaw angle yields

$$\varepsilon = \frac{\sqrt{1 - 1/S_g}}{(2I_y / I_x - 1)} \sin \delta_{\max} \quad (8)$$

Substituting Eq. (8) into Eq. (6) yields a mean of predicting the in-bore yaw angle resulting from CT ammunition chamber misalignment based on the mean impact point observed at the target

$$J_A = -i \left(\frac{2\pi}{n} \right) \left(\frac{C_{L\alpha}}{C_{M\alpha}} \right) \sin \left(\frac{\sqrt{1 - 1/S_g}}{(2I_y / I_x - 1)} \sin \delta_{\max} \right) e^{i\phi_0} \quad (9)$$

In addition to the aerodynamic jump component, there is a lateral throw-off component that arises because of the in-bore yaw angle of the projectile. Referring to Fig. 1, and assuming that the projectile tilt occurs at the mid-point of the cylindrical portion of the projectile, then there will be a static unbalance if the center

of mass is located either ahead of or aft of the mid-point.

The relationship between the static unbalance and the tilt angle is given by McCoy [8] as follows

$$\frac{\hat{\varepsilon}}{d} = \left(L_N + \frac{1}{2} L_{CYL} - CG_N \right) \sin \varepsilon \quad (10)$$

The lateral throw-off due to the bullet tilt at the muzzle is computed using the following equation derived in McCoy [8]

$$T_L = i \left(\frac{2\pi}{n} \right) \left(\frac{\hat{\varepsilon}}{d} \right) e^{i\phi_0} \quad (11)$$

$$T_L = i \left(\frac{2\pi}{n} \right) \left(\frac{\hat{\varepsilon}}{d} \right) e^{i\phi_0}$$

Substituting Eq. (10) into Eq. (11), one gets the lateral throw-off due to the in-bore bullet tilt

$$T_L = i \left(\frac{2\pi}{n} \right) \left(L_N + \frac{1}{2} L_{CYL} - CG_N \right) \sin \varepsilon e^{i\phi_0} \quad (12)$$

Both the aerodynamic jump and the lateral throw-off can be related to the first maximum yaw angle as follows

then be added to obtain the total projectile deflection resulting from the chamber misalignment. This will be shown in the Results and discussion section.

3. Experimental setup and procedure

Tests were performed in the DRDC aeroballistic range. This is an indoor firing range that allows for accuracy and precision trials under controlled environmental conditions. The distance to the target was set at 200 m. The

$$\sin \delta_{\max} = \left(2 \frac{I_y}{I_x} - 1 \right) \left(\frac{\varepsilon}{\sqrt{1 - I_y/I_x}} \right) \quad (7)$$

projectile velocity was measured over the whole trajectory using a Doppler radar. The average muzzle velocity for rounds fired was determined to be

944.9 m/s. The center of the field of view of two orthogonal high-speed cameras was positioned at 0.9 m from the muzzle of the barrels. These orthogonal projectile images were combined to extract the projectile first maximum yaw angle required for the data analysis.

The aeroballistic range and the firing position including the accuracy test fixture, test stand and the two high-speed cameras are shown in Fig. 2.

The Mann barrel and the CT ammunition chamber were mounted on a derivative of the standard NATO accuracy test

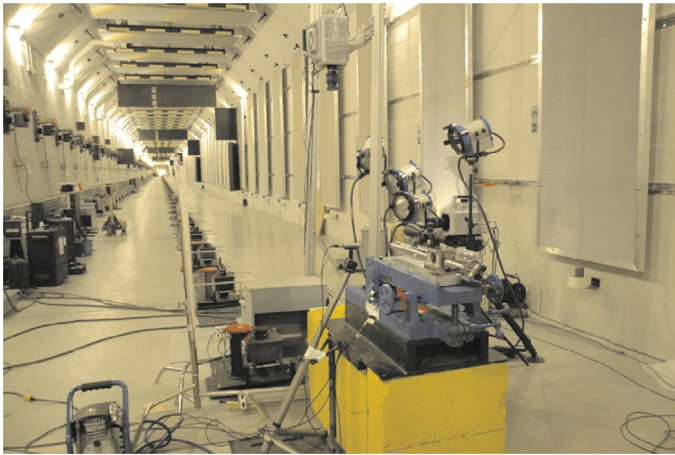


Fig. 2. Accuracy test fixture, test stand and the two high-speed cameras (circled).

fixture. A close-up view is shown in Fig. 3. The barrel length was 18 inches (457 mm). The accuracy test fixture was designed to ensure that it had minimum impact on bullet dispersion. This was done through two means: properly restraining barrel movement and soft mounting the test fixture on the main test stand. The barrel was held at two points: near the muzzle and near the chamber. Near the muzzle, lateral movement was constrained. However, movement was permitted in the axial direction to account for potential barrel heating. Near the chamber the barrel was fixed with no movement permitted. Soft mounting of the accuracy test fixture was accomplished through the use of two parallel rods and a spring-damper system. Movement was permitted along the axial direction thereby distributing over time the recoil forces experienced by the barrel. The accuracy fixture was mounted on a test stand that was sufficiently heavy that it did not move as a result of the firing event. For this project, 5.56 mm CT ammunition was used as shown in Fig. 4. All ammunition was conditioned to 21 °C. The barrels were not conditioned.

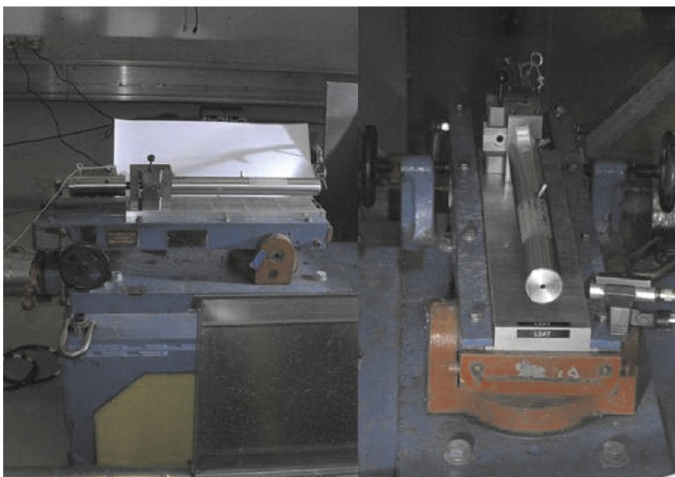


Fig. 3. Close-up view of the test stand and the Mann barrel.

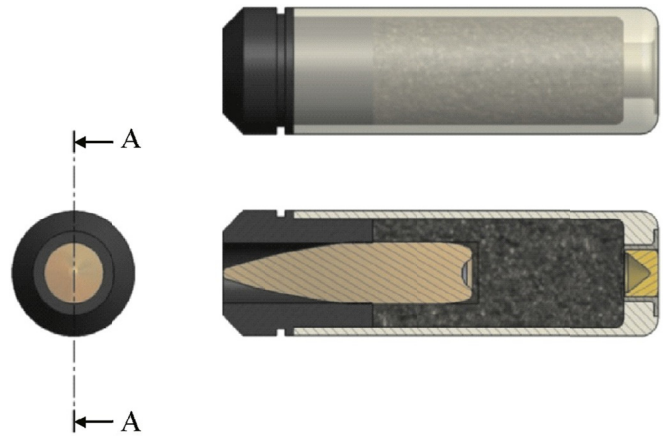


Fig. 4. Cut-away drawing of the 5.56 mm CT ammunition.

For each barrel test series, point of aim was adjusted using a bore sight laser. A Leupold MK 4 LR/T 6.5 × 20 × 50 mm optical sight was used to ensure that the fixture did not move from one firing to the next. No movement was observed throughout the firings.

The Doppler radar, an OPOS ED1000, was mounted slightly behind and to the left of the test fixture. It measured the bullet velocity along the total flight path.

A paper target (Fig. 5) was used which could be advanced after each series. Bullet point of impact was evaluated using an optical measuring system. A high resolution photo of the target was taken after each shot by a camera placed in front of the target. The image was downloaded immediately to a computer program where a technologist selected the point of impact with a cursor. Measurement accuracy using this system was ± 1 mm.

In order to perform this study, a breech block was designed with a cylindrical chamber as shown in Fig. 6. In addition to the baseline chamber which is concentric with the Mann barrel bore, six additional chambers were manufactured with an offset relative to the barrel bore. Three chambers were manufactured

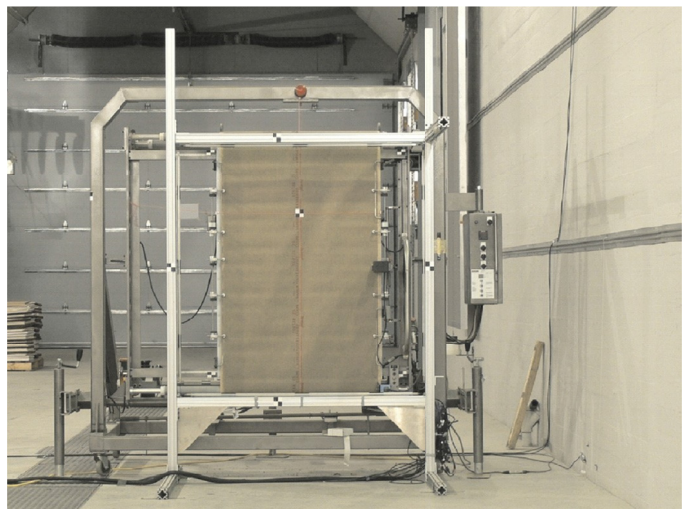


Fig. 5. Paper target system.

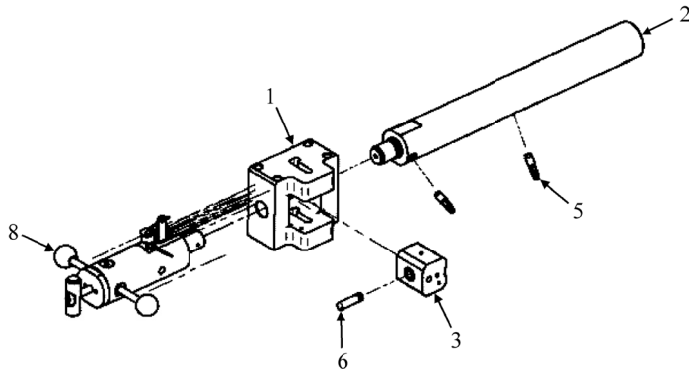


Fig. 6. CT ammunition Mann-barrel drawing. Parts: 1 – central block; 2 – barrel; 3 – chamber; 5 – Kistler pressure transducer; 6 – CT round; 8 – firing pin system.

with rightward misalignments of 0.010 inch (0.254 mm), 0.015 inch (0.381 mm) and 0.020 inch (0.508 mm) respectively. Thus, when looking from being the mount, the chamber axis is to the right of the barrel axis. Similarly, three chambers were manufactured with upward misalignments of 0.010 inch (0.254 mm), 0.015 inch (0.381 mm) and 0.020 inch (0.508 mm) respectively. Thus, when looking from being the mount, the chamber axis is above the barrel axis for these cases.

The test matrix followed during the trial is shown in Table 1. One series of 30 rounds was fired for each configuration except for the standard configuration for which 2 series were fired. For all of these 30 rounds attempted, some misfires occurred such that, in the end, each series consisted of less than 30 impact points.

4. Results and discussion

Precision and accuracy tests were performed at 200 m in an indoor range under controlled conditions for the baseline chamber and the six additional chambers with an offset. For this project, 5.56 mm CT ammunition was used. The mean impact point for each chamber tested is shown in Fig. 7. Each point in Fig. 7 corresponds to one of the series listed in Table 1.

As seen from this figure, as the chamber axis offset relative to the gun bore is increased, the mean point of impact is moved to the right for the horizontally offset chamber and upward for the vertically offset chamber. The shift in the impact location can be explained by the presence of in-bore yaw which results

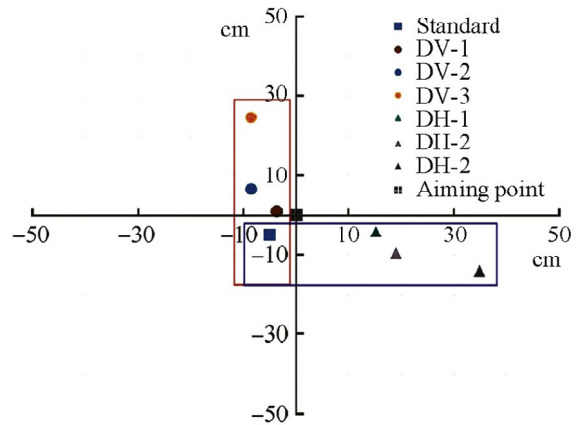


Fig. 7. Mean point of impact of CT ammunition at 200 m, as fired from seven different chambers. DV-1, DH-1: 0.010 inch offset; DV-2, DH-2: 0.015 inch offset; DV-3, DH-3: 0.020 inch offset.

in a lateral throw-off and an aerodynamic jump component. However, the fact that the mean point of impact (MPI) is displaced in the same direction as the chamber offset (vertically or horizontally) cannot be explained physically. It is believed that if the barrel had been slightly longer or shorter, the MPI would have been in a direction different from the chamber displacement. This will be verified in a follow-up study by cutting the barrel down to various lengths and repeating the firing at each length. The MPI shifts outward from the target center with increased chamber offset because the aerodynamic jump and the lateral throw-off increase due to a larger in-bore yaw. As the tilted projectile moves down the barrel, the projectile in-bore yaw angle orientation constantly changes following the barrel twist rate. Thus, for a given misaligned chamber, a slightly longer or shorter barrel would have given a different direction for the MPI shift.

In order to correlate the MPI shift to the chamber offset, the first-max yaw angle was required. As mentioned previously, two high-speed orthogonal cameras located at 0.9 m from the muzzle were used to obtain the pitch and the yaw of the projectile. An example is shown in Fig. 8 for the fourth firing made with the second horizontally offset chamber DH-2. The first maximum yaw angle is found by combining the angle measured in the yaw plane and the pitch in the pitch plane. The approximate location of the first maximum yaw along the trajectory is

Table 1
Test matrix.

Configuration	Axial misalignment of the chamber/inches	Temperature/°C	Number of series of 30 shots	Measured parameters
Standard CT	0.000	+21	2	D,MV,Y&P
DH-1(#1)CT	0.010 horizontally	+21	1	D,MV,Y&P
DV-1(#2)CT	0.010 vertically	+21	1	D,MV,Y&P
DH-2(#3)CT	0.015 horizontally	+21	1	D,MV,Y&P
DV-2(#4)CT	0.015 vertically	+21	1	D,MV,Y&P
DH-3(#5)CT	0.020 horizontally	+21	1	D,MV,Y&P
DV-3(#6)CT	0.020 vertically	+21	1	D,MV,Y&P

DH: displaced horizontally; DV: displaced vertically; D: dispersion measured; MV: muzzle velocity measured; Y&P: projectile yaw and pitch, estimated from the high speed camera photos.

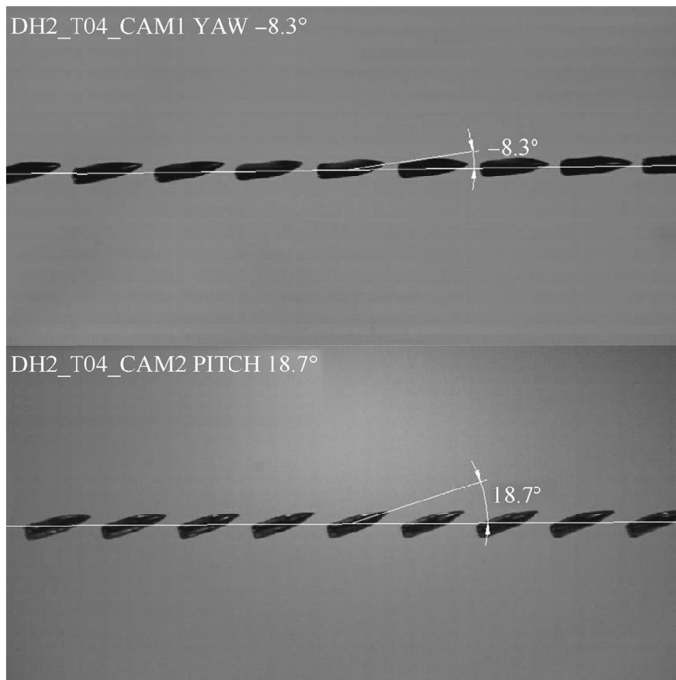


Fig. 8. High-speed video image used to extract the first maximum yaw angle of the projectile after the muzzle exit.

approximately known prior to testing from prior knowledge of the projectile physical and aerodynamic properties. As seen from Table 2, the magnitude of the first maximum yaw correlates with the chamber misalignment both in the vertical and horizontal directions.

The values of the projectile aerodynamic and physical parameters required to compute the aerodynamic jump associated with the projectile in-bore tilt are tabulated in Table 2.

Referring to Fig. 1 in order to compute the lateral throw-off associated with the 5.56 mm CT projectile tilt, the following parameters are required (in caliber)

$$L_N = 2.13 \text{ cal}$$

$$L_{CYL} = 1.56 \text{ cal}$$

$$CG_N = 2.58 \text{ cal}$$

The computed deflections for the various test cases are shown in Table 3. For these calculations, the initial roll angle, ϕ_0 , for the projectile was not available experimentally. However, using a high-fidelity 6-DOF model of the 5.56 mm projectile, it was possible to determine the initial roll angle that yielded the experimentally determined first maximum yaw. An initial roll angle, ϕ_0 , very close to 180° was determined for the horizontally offset chamber, whereas initial roll angle, ϕ_0 , very close to 270° was determined for the vertically offset chamber. A comparison between the experimentally determined MPI and the theoretically determined MPI is shown in Fig. 9. Although the comparison is not perfect, the general trend in the deflection of the MPI is well picked up by theoretical model. The discrepancies could be due to the rough approximation made when estimating the static unbalance of the projectile due to the projectile tilt. Furthermore, the MPI were determined using a single sample of less than 30 rounds due to the misfired rounds. Additional firing could possibly yield slightly different MPI.

5. Conclusion

An analytical method based on the linear theory of ballistics was developed to evaluate the influence of a CT ammunition rifle chamber misalignment on the mean point of impact location of a grouping from that same rifle. The results indicate that

Table 2

Physical and aerodynamic properties used to compute the aerodynamic jump for the various chamber configurations.

Chamber	Axial misalignment of the chamber/inches	MPI in x/cm	MPI in y/cm	First max yaw angle/(°)	S_g	$\frac{I_y}{I_x}$	$C_{L\alpha}$	$C_{M\alpha}$	k_y^2	k_x^2	N (cal/rev)	Muzzle velocity/(m·s ⁻¹)
Standard CT	0.000	-5.0	-5.1	1.55	2.41	8.55	2.53	2.39	0.9273	0.1085	32	938.2
DH-1(#1)CT	0.010 horizontally	15.3	-4.2	5.00	2.41	8.55	2.53	2.39	0.9273	0.1085	32	943.1
DV-1(#2)CT	0.010 vertically	-3.7	1.0	5.31	2.41	8.55	2.53	2.39	0.9273	0.1085	32	942.5
DH-2(#3)CT	0.015 horizontally	19.1	-9.4	16.19	2.41	8.55	2.53	2.39	0.9273	0.1085	32	948.7
DV-2(#4)CT	0.015 vertically	-8.6	6.6	11.58	2.41	8.55	2.53	2.39	0.9273	0.1085	32	947.6
DH-3(#5)CT	0.020 horizontally	34.9	-14.0	19.69	2.41	8.55	2.53	2.39	0.9273	0.1085	32	948.2
DV-3(#6)CT	0.020 vertically	-8.6	24.6	20.78	2.41	8.55	2.53	2.39	0.9273	0.1085	32	946.1

Table 3

Computed deflection for the different configurations.

Chamber	Axial misalignment of the chamber/inches	J_A	T_L	Deflection due to J_A /cm	Deflection due to T_L /cm	Total deflection/cm
Standard CT	0.000	0.000219	-8.308E-05	4.37	-1.66	2.71
DH-1(#1)CT	0.010 horizontally	0.000705	-0.0002676	14.09	-5.35	8.74
DV-1(#2)CT	0.010 vertically	0.000748	-0.0002842	14.97	-5.68	9.28
DH-2(#3)CT	0.015 horizontally	0.002254	-0.0008563	45.09	-17.13	27.96
DV-2(#4)CT	0.015 vertically	0.001623	-0.0006165	32.46	-12.33	20.13
DH-3(#5)CT	0.020 horizontally	0.002724	-0.001034	54.48	-20.70	33.79
DV-3(#6)CT	0.020 vertically	0.002868	-0.001089	57.37	-21.79	35.58

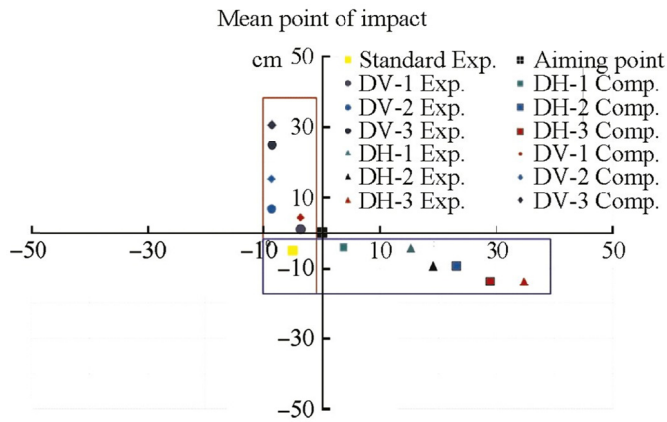


Fig. 9. Comparison between the experimental MPI and the theoretically computed MPI.

the model can indeed predict the trend correctly. The theoretical relationship could certainly be used to diagnose chamber misalignment or used to set specification on the maximum allowable chamber misalignment for a manufacturer. It is believed that the difference between the experimental results and the theoretical model predictions are mainly due to the small firing sample used to obtain the experimental mean point of impact. Another source of discrepancy is probably due in part to the geometric relationship used to estimate the static imbalance.

Future work that could be performed to improve the theoretical prediction includes the development of a geometrical

relationship to predict the projectile in-bore tilt based on chamber misalignment. Furthermore, additional firing should be performed to improve the confidence in the experimental mean point of impact. Finally, in a subsequent trial, orthogonal cameras should be positioned at the muzzle of the gun in order to extract experimentally the initial roll position of the projectile instead of relying on 6-DOF simulations.

References

- [1] Shipley PA, Cole BT, Phillips K. Cased telescoped small arms systems. Presented at the Joint armaments forum, exhibition & technology demonstration, Phoenix, AZ, 12–15 May; 2014.
- [2] Mann FW. The bullet's flight from powder to target. New York, NY: Munn & Company; 1909.
- [3] Murphy CH. Yaw induction by mass asymmetry. *J Spacecr Rockets* 1977;14(8):511–12.
- [4] Ritter JJ. Barrel leade effects on 5.56 mm interior ballistics. In: Proceedings of the 28th international symposium on ballistics, Atlanta, GA, 22–26 September; 2014.
- [5] Bayer RA, Ritter JJ. Measurements of early bullet motion at 5.56 mm and 7.62 mm. In: Proceedings of the 28th international symposium on ballistics, Atlanta, GA, 22–26 September; 2014.
- [6] Gkritzapis DN, Panagiotopoulos EE. In-bore yaw effects on lateral throw-off and aerodynamic jump behaviour for small caliber projectiles firing sidewise from air vehicles. *J Appl Mech* 2011;78(5):051017.
- [7] Murphy CH. Free-flight motion of symmetric missiles. Ballistic Research Laboratories Report No. 1216; 1963.
- [8] McCoy RL. Modern exterior ballistics: the launch and flight dynamics of symmetric projectiles. Atglen, PA: Schiffer Publisher; 1998.
- [9] McShane EJ, Kelley JL, Reno FV. Exterior ballistics. Denver, CO: University of Denver Press; 1953.